Total Neutron Cross Section Measurement on CH with 3D Projection Scintillator Detector

Eric Chong
on behalf of
3D Projection Scintillator R&D Group
BNL Seminar
November 10th 2022

3D Projection Scintillator R&D group

CERN
Chung-Ang University, South Korea
ETH Zurich, Switzerland
University of Geneva, Switzerland
High Energy Accelerator Research Organization (KEK), Japan
IFAE (Spain)
Imperial College, UK
Institute for Nuclear Research (INR), Russia
University of Kyoto, Japan
Louisiana State University
University of Pennsylvania
University of Pittsburgh
University of Rochester
South Dakota School of Mines and Technology
Stony Brook University
University of Tokyo, Japan

Motivation

- Neutron detection and reconstruction are not accessible with current particle detector technology
- Neutron information remains as one of the major missing piece in the energy reconstruction for anti-neutrino → Among the largest uncertainty in NOvA

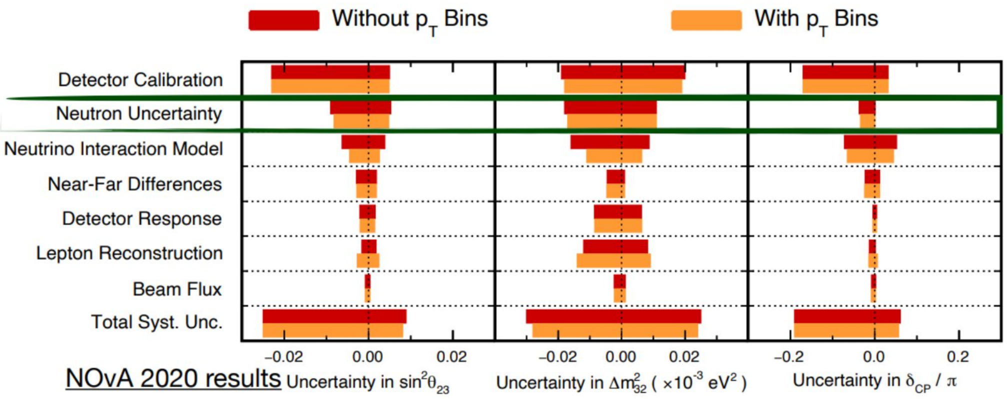

NOvA 2020 results

Motivation

- 3D projection scintillator technology not only enables neutron detection but also reconstruction of neutron kinematics on an **event-by-event** basis
  - Will be used in near detector for T2K (SuperFGD)
  - Proposed near detector for DUNE (3DST)
- Increased availability of neutron information helps to reduce uncertainty on anti-neutrino energy reconstruction → Improve the constraints on the flux and cross section uncertainties for the oscillation analysis

ND280 Upgrade

- SuperFGD as main target
- 2 TPCs top and bottom of SuperFGD
- 6 Time-of-Flight detectors cover the SuperFGD and high-angle TPCs

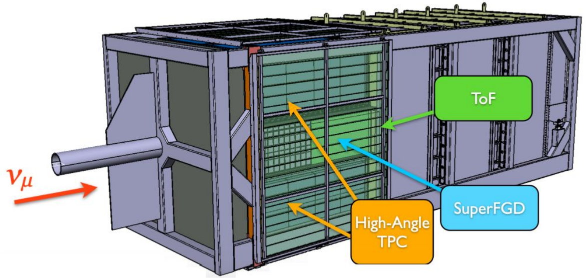

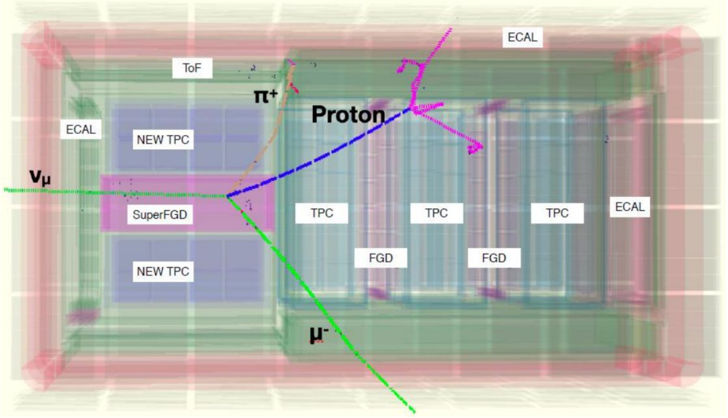

SuperFGD

- 3D array of 1 cm^3 scintillator cubes (fine-grained detector)
- 3D readout with 3 WLS fibers passing through each cube and connected to MPPCs (multi-pixel photon counters)

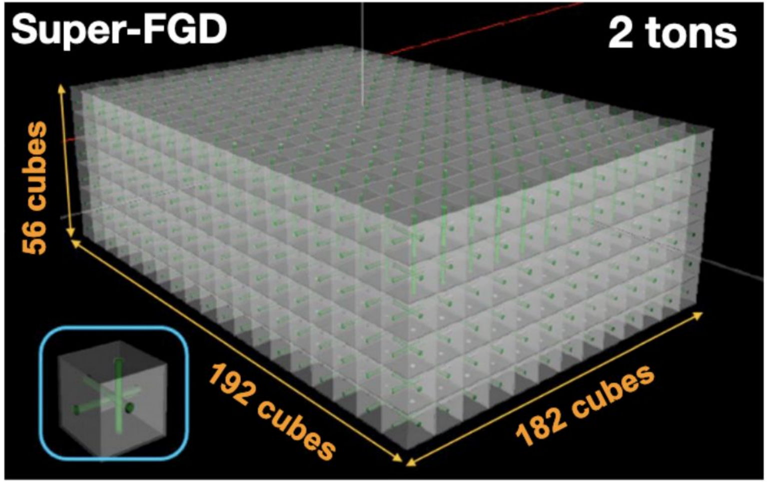

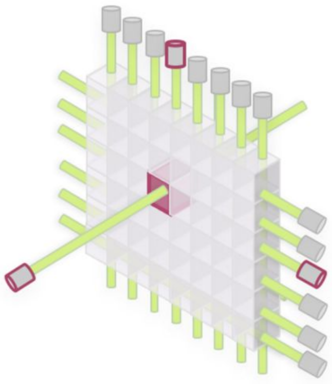

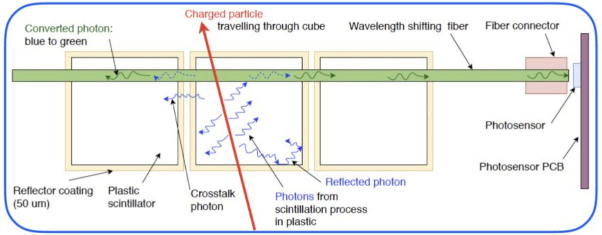

2018 JINST 13 P02006 NIM A936 (2019) 136-138

SuperFGD

- Increased target mass (2 tons)
- Improved uniformity of detection efficiency as function of angle
- Improved detection efficiency for transverse particles
- Lower detection threshold for protons
- Capable of measuring neutron kinematics using time-of-flight internal to the detector (see here)

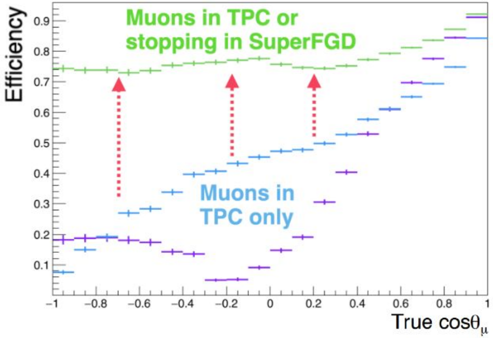

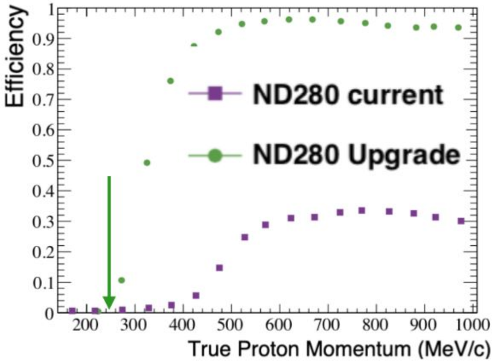

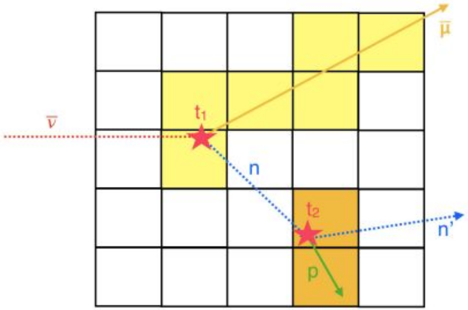

SuperFGD Status

- Cubes (produced and assembled at INR) and mechanical box (assembled and tested at CERN) shipped to Japan
- Detector assembly on-going in Japan
- MPPC boards fabricated and currently being tested at LSU and U. Tokyo
- Front-end electronics currently in production and full vertical slice test to be conducted later this year
- First neutrino data in 2023

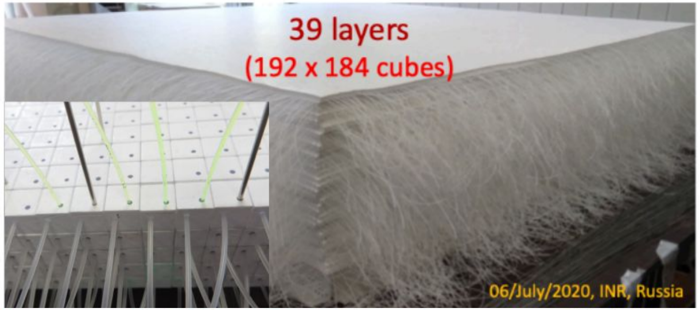

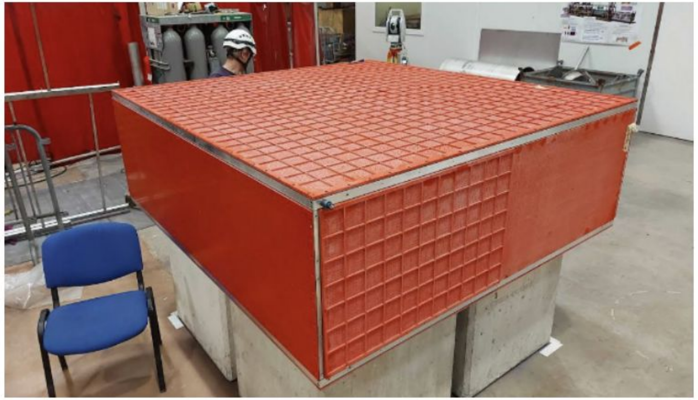

SuperFGD Prototype

- Prototype detector developed and exposed to charged particle beams (p and π) at CERN in 2018
- Good performances observed from beam tests:
  - Average light yield of 58 PE per MIP per cube
  - 3% cube-to-cube optical crosstalk
  - 0.97 ns single channel time resolution (see here)
  - Good particle identification

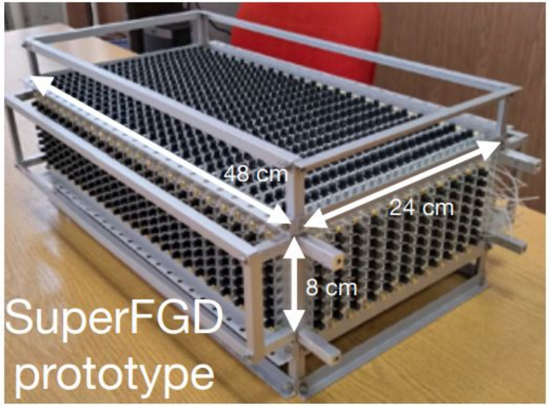

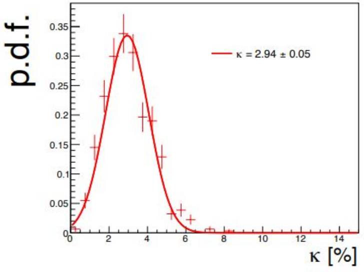

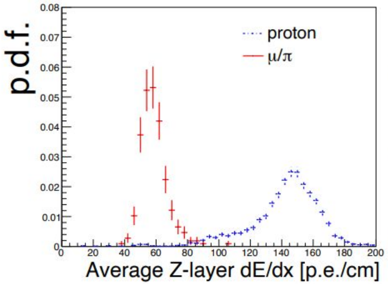

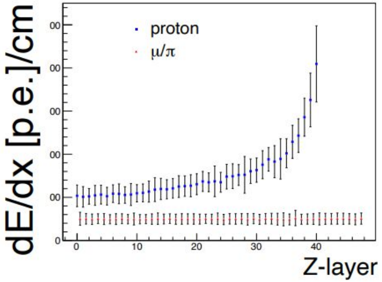

A. Blondel et al 2020 JINST 15 P12003

SuperFGD Prototype

- Prototype detector deployed at LANL for neutron beam test in 2019
- Main purpose: Characterization of prototype detector (same technology as SuperFGD and 3DST) performance and response to neutrons
  →Total n-CH cross section as first analysis

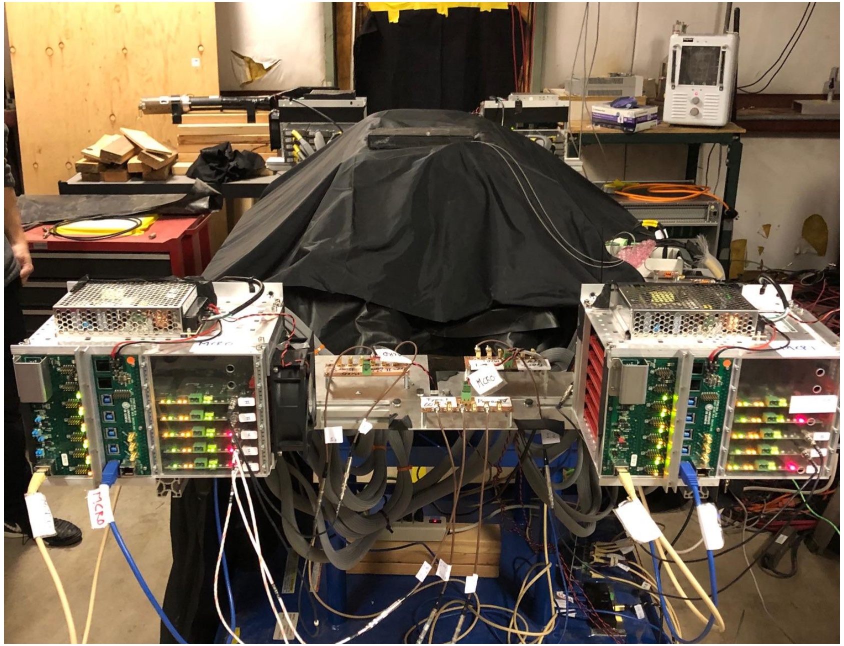

SuperFGD Prototype

- Various calibration runs taken before accepting neutron beam
  - LED runs for channel-by-channel gain calibration (temperature variation included)
  - Cosmic samples for channel-by-channel light yield calibration (PE per MeV)

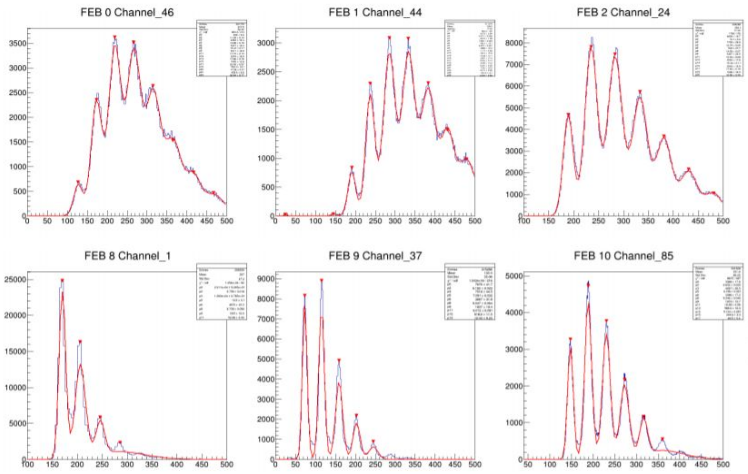

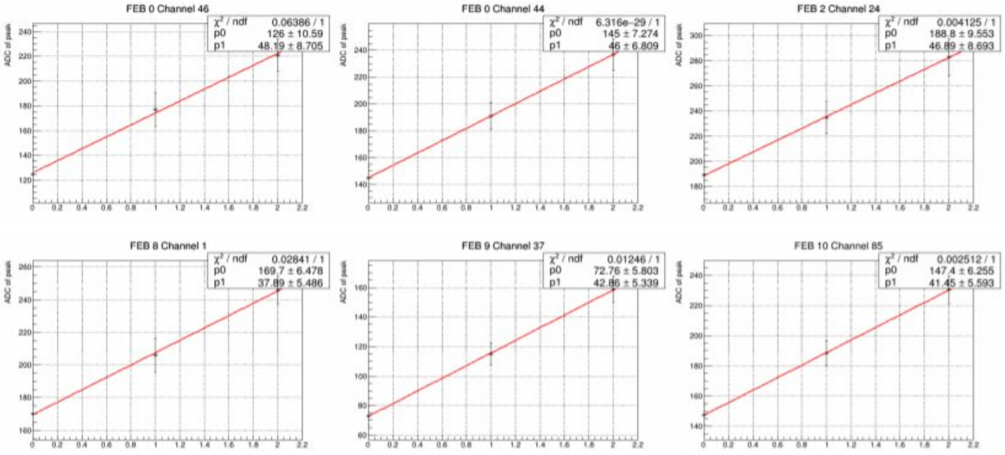

LANL Facility

- Neutron beam data taken at the 90 m location (15L) for around 2 weeks
- WNR able to provide neutron beam ranged from 0 to 800 MeV

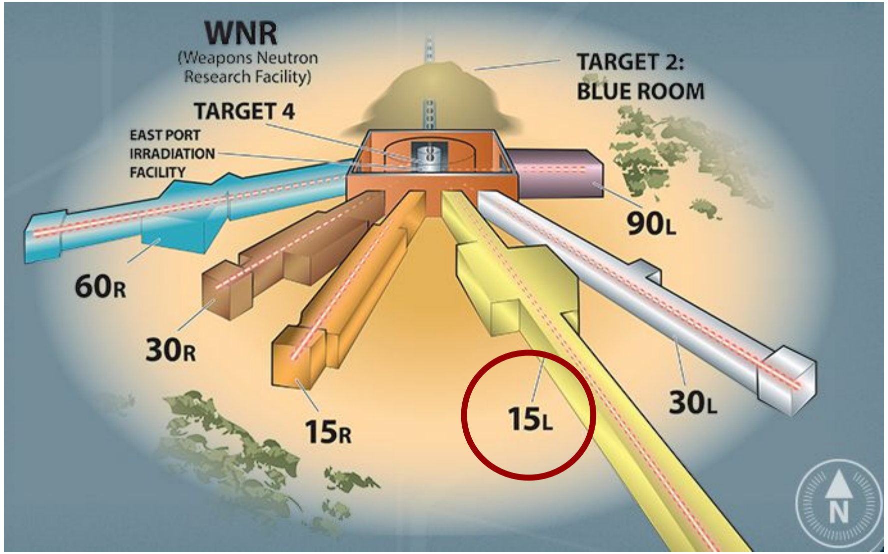

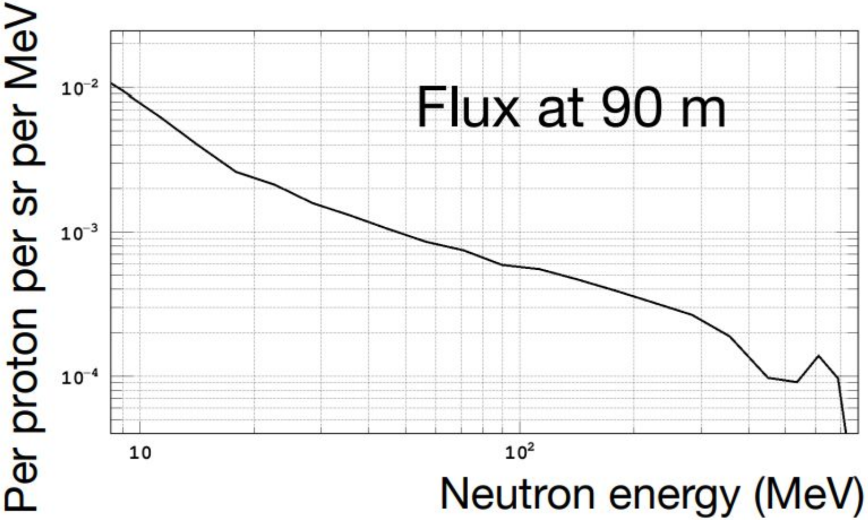

LANL Neutron Beam

- Proton bunch spacing of 1.8 us (micropulse)
  - Proton bunch width of a few hundred picoseconds (smaller than time resolution of prototype detector)
  - Spread in neutron arrival time (as seen by detector) is due to different neutron kinetic energy (not due to different neutron production time)

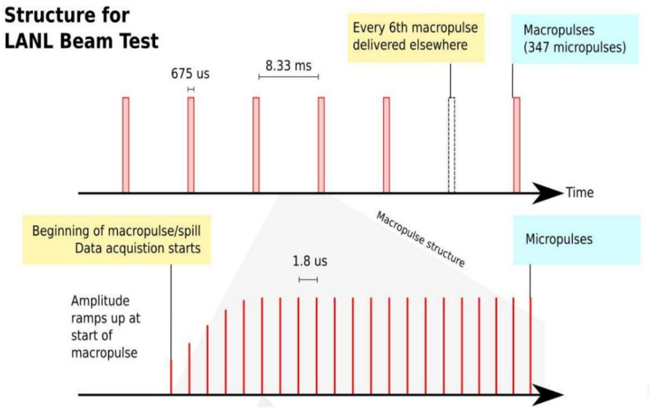

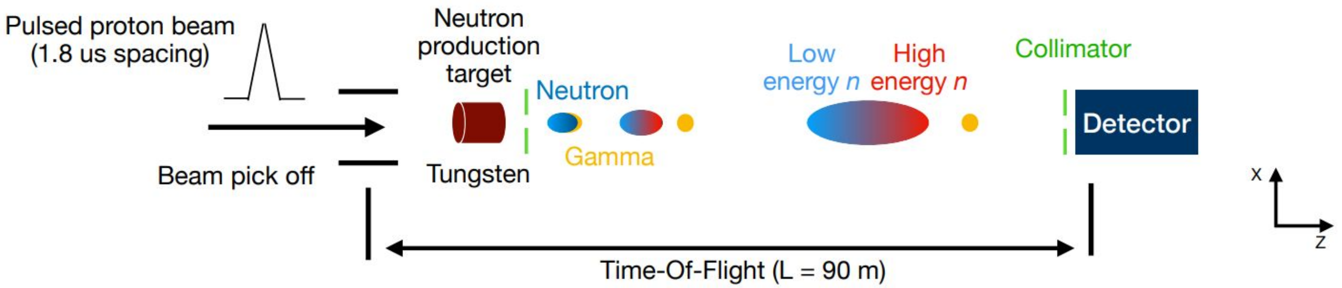

LANL Neutron Beam

- Neutron energy measured on an event-by-event basis using time-of-flight (ToF) method with **t0** signal provided by beamline

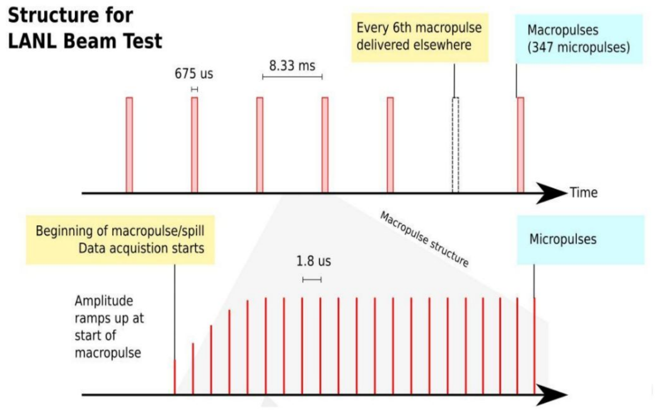

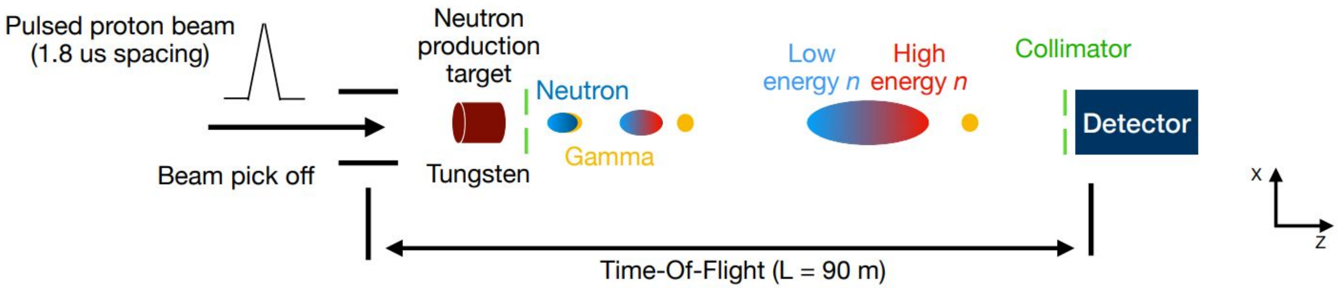

LANL Neutron Beam

- What we see in the detector:

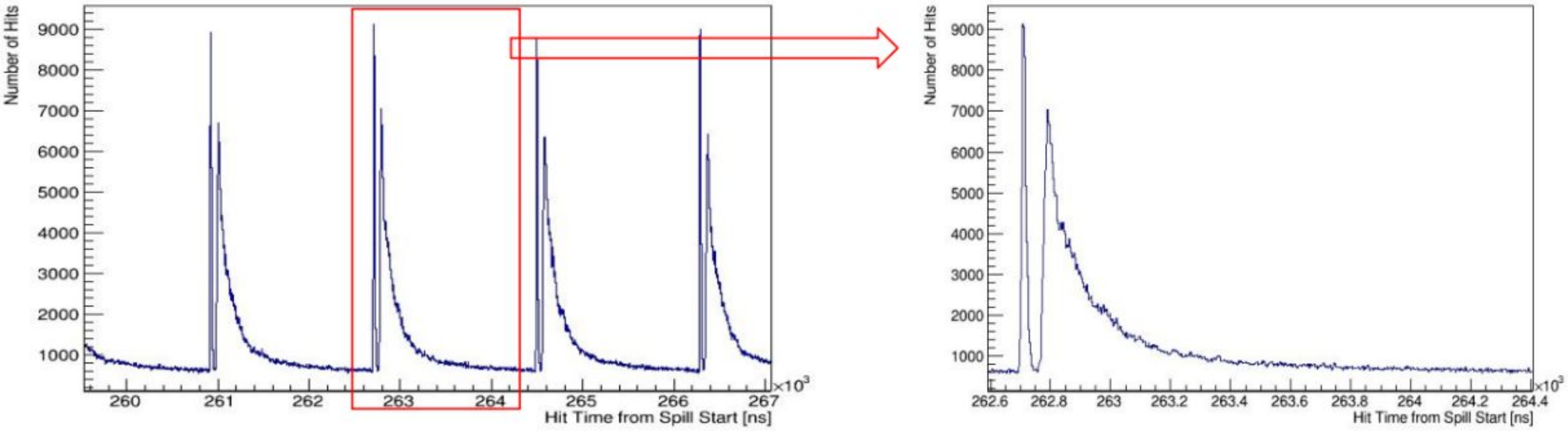

LANL Neutron Beam

- What we see in the detector: Gamma flash arrives before neutron

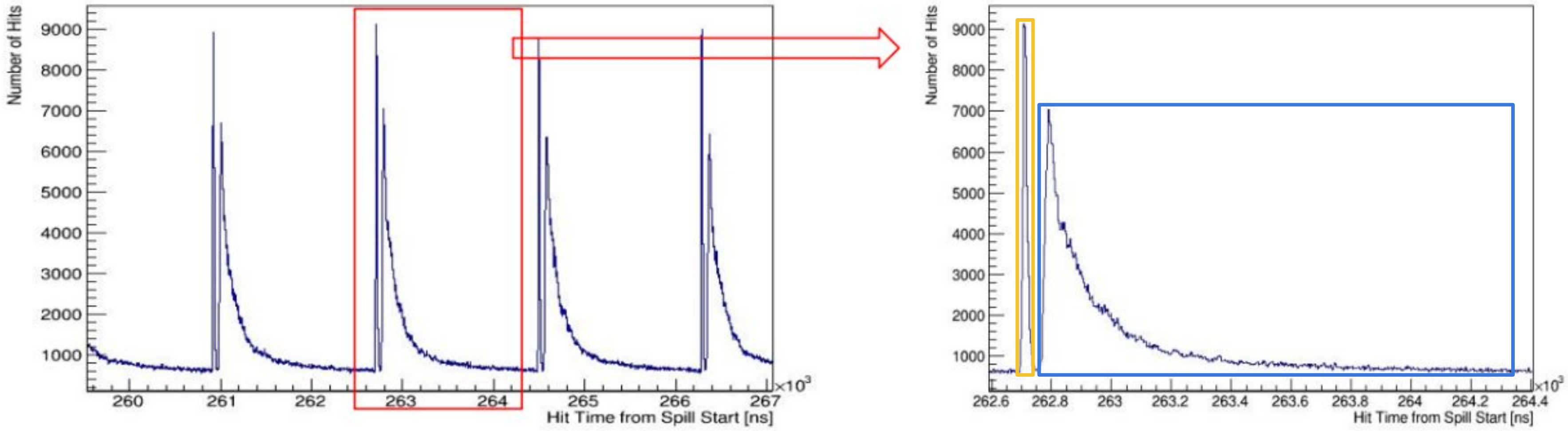

Total n-CH Cross Section

- Total neutron cross section on CH measurement has been obtained using data taken in 2019 (submitted to ArXiv recently)
- Measurement strategy:
  - Neutron flux decreases as a function of depth in the detector due to neutron interactions with CH
  - The total neutron-CH cross section can be extracted from the attenuation of the beam $N_0 e^{-T\sigma z}$
  - The attenuation can be measured by choosing a particular event topology and measuring the change in the rate of the chosen topology as a function of depth in the detector
  - The fraction of the total cross section that results in the chosen topology is assumed to be constant as a function of depth
  - We have chosen **events with single reconstructed tracks** as topology

Event Reconstruction

2D Hits

- Time cut on hits
- Gain re - calibration
- PE cut on hits
- Time-walk correction
- Time clustering hits

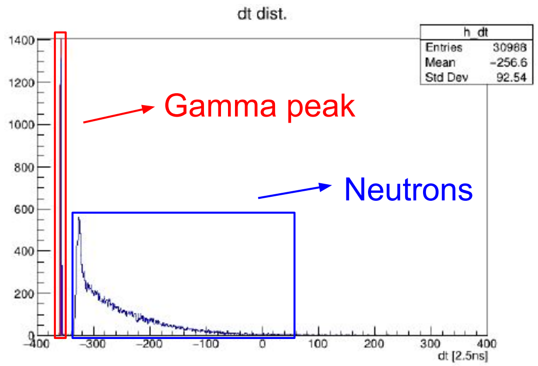

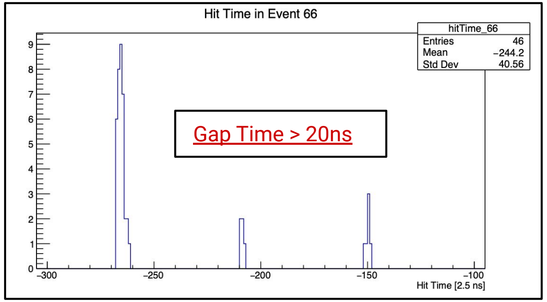

Event Reconstruction

2D Hits	3D Voxels
Time cut on hits Gain re - calibration PE cut on hits Time-walk correction Time clustering hits	3D view matching of time - clustered hits 3 hits sharing the same XYZ coordinates Attenuation correction with variable PE cut

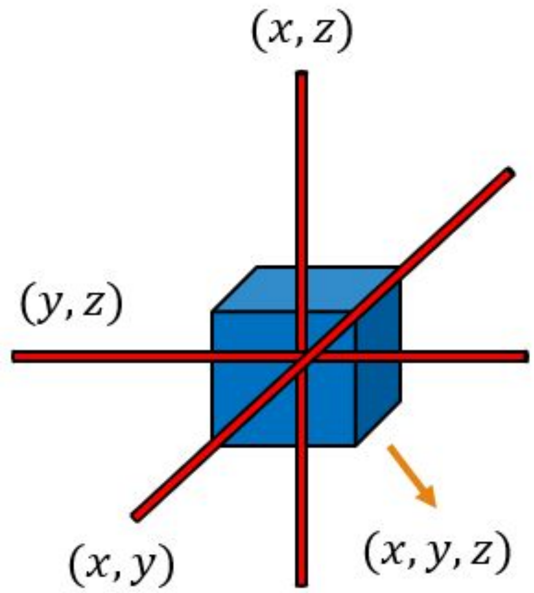

Event Reconstruction

2D Hits	3D Voxels	Clusters
Time cut on hits Gain re - calibration PE cut on hits Time-walk correction Time clustering hits	3D view matching of time - clustered hits 3 hits sharing the same XYZ coordinates Attenuation correction with variable PE cut	DBSCAN clustering of voxels Maximum distance of 1.8 cm between voxels in the same cluster

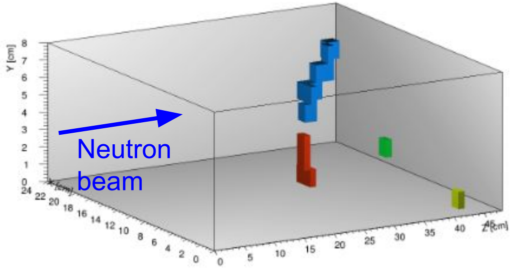

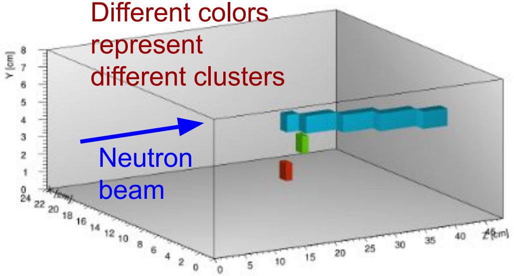

Single Track Event Selection

Single time cluster of hits

↓

Single DBSCAN cluster of voxels

↓

3 - 8 number of voxels in single cluster

↓

Single Track Event Selection

Single time cluster of hits

↓

Single DBSCAN cluster of voxels

↓

3 - 8 number of voxels in single cluster

↓

Linearity > 0.70

↓

Linearity:

- Obtained with PCA (Principal Component Analysis) calculation
- Calculate the centroid for a distribution of points
- Calculate the covariance matrix with the centroid

$$[Cov]_{ij} = \frac{\sum_{l=1}^{N}(A_i - \overline{A_i}) \cdot (A_j - \overline{A_j})}{N}$$

- Perform eigen decomposition on the covariance matrix to obtain the eigenvalues of the covariance matrix
- Sort the obtained eigenvalues by $\lambda_1 \geq \lambda_2 \geq \lambda_3 \geq 0$
- Evaluate the linearity, planarity and sphericity of the distribution of points

Linearity	$(\lambda_1 - \lambda_2)/\lambda_1$
Planarity	$(\lambda_2 - \lambda_3)/\lambda_1$
Sphericity	λ_3/λ_1

Single Track Event Selection

Single time cluster of hits

↓

Single DBSCAN cluster of voxels

↓

3 - 8 number of voxels in single cluster

↓

Linearity > 0.70

↓

Cluster width < 1.4 and max-vox-line < 1.2

↓

Cluster width:

- 1D projection of voxels to the eigenvector with the second largest eigenvalue (from PCA calculation)

  $d_i = \boldsymbol{v_2} \cdot (\boldsymbol{r_i} - \bar{\boldsymbol{r}})$

  $\boldsymbol{v_2}$: *Eigenvector with the second largest eigenvalue*

  $\boldsymbol{r_i}$: *3D coordinate of voxel i*

  $\bar{\boldsymbol{r}}$: *Mean 3D coordinate of voxels in the same cluster*

- Calculate the distance (cluster width) between the 2 voxels furthest away from each other in this eigenbasis:

$$d = d_{max} - d_{min}$$

Cluster width = 0

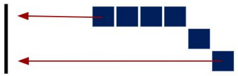

Cluster width ≈ 2

Single Track Event Selection

Single time cluster of hits

↓

Single DBSCAN cluster of voxels

↓

3 - 8 number of voxels in single cluster

↓

Linearity > 0.70

↓

Cluster width < 1.4 and max-vox-line < 1.2

↓

Max-vox-line:

- Calculate the eigenvectors for a cluster of voxels using PCA
- First eigenvector which is the eigenvector with the largest eigenvalue (red line in the figure) gives the direction of the best fit line

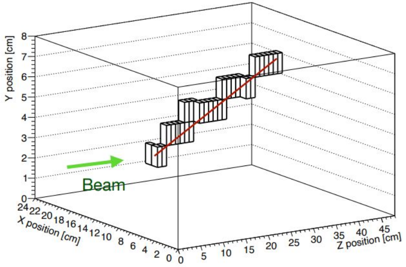

- Compute the maximum distance (max-vox-line) between the voxels and the first eigenvector

Single Track Event Selection

Single time cluster of hits

↓

Single DBSCAN cluster of voxels

↓

3 - 8 number of voxels in single cluster

↓

Linearity > 0.70

↓

Cluster width < 1.4 and max-vox-line < 1.2

↓

Vertex in fiducial volume (1.5 cm radius around beam center) and not in first layer in Z (Z > 0)

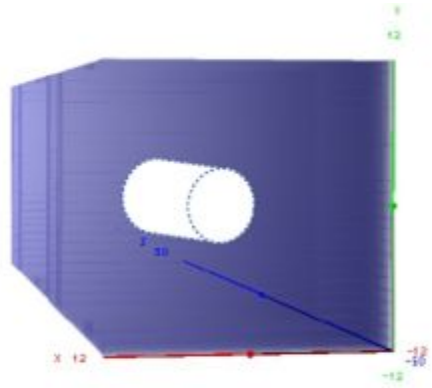

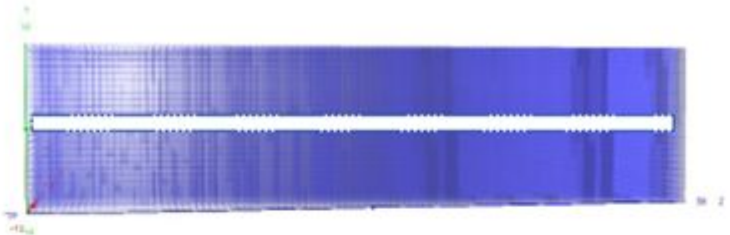

Cross Section Fitter

- Fill an histogram for every energy (from ToF between production point and vertex) bin which is the distribution of the number of events as function of the depth (z-layer)
- Energy binning optimized taking into account the time-tick resolution (2.5 ns)
- Energy restricted to be between 98 and 688 MeV
  - < 98 MeV: Tracks not long enough and increased neutron elastic scattering
  - > 688 MeV: Much less statistics and increased contamination from gammas
- Fit with the exponential $N_0 e^{-T\sigma z}$
- Extract the cross section for every bin from the exponential fit

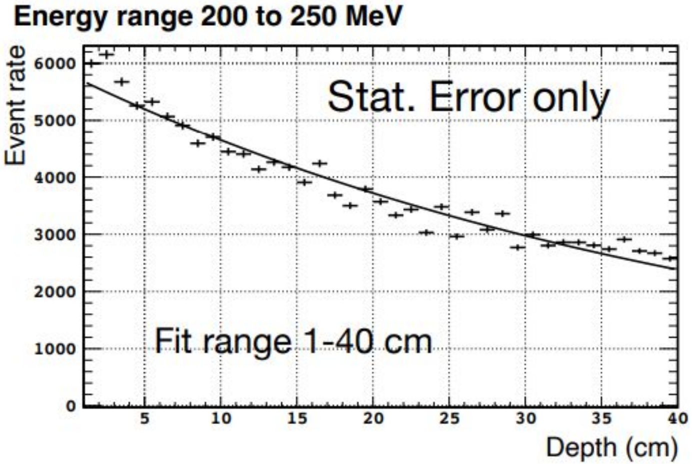

Cross Section Systematics

- Time resolution
- Invisible scattering
- Detector effects
- Geometric acceptance
- Light yield
- Collimator interaction

Cross Section Systematics

Time resolution:

- Randomly smear the timing around nominal within a gaussian with a sigma of 1.37 ns time resolution (obtained here)
- Once a new set of shifted events is created, fit the shifted events to produce shifted extinction plots
- Repeat for a number of times and get distribution of extinction parameters
- Sigma of that distributions as the systematic error

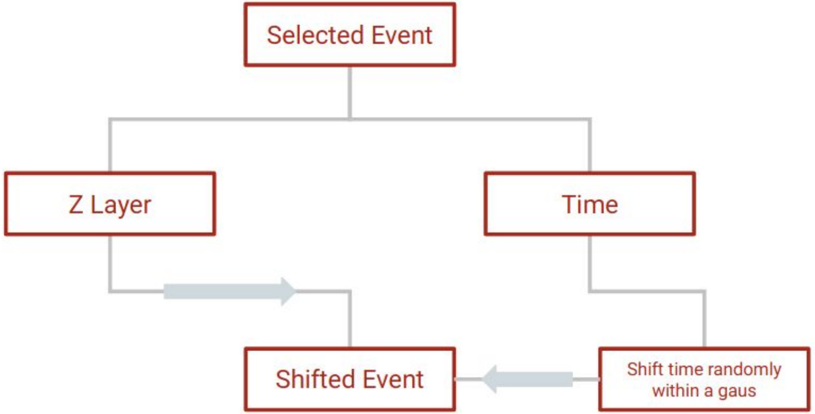

Cross Section Systematics

Invisible scattering:

- Undetected neutron interactions introduce a smearing to the neutron energy estimation
- The invisible scattering mainly cause a displacement of the vertex
- Transverse spread of the beam used to characterize such scattering
- Tuned transverse spread in MC (Geant4 Bertini and INCLXX lists) to data assuming it was all due to invisible scattering (very conservative)
- 2% of invisible scattering for energy > 98 MeV is taken as systematic error

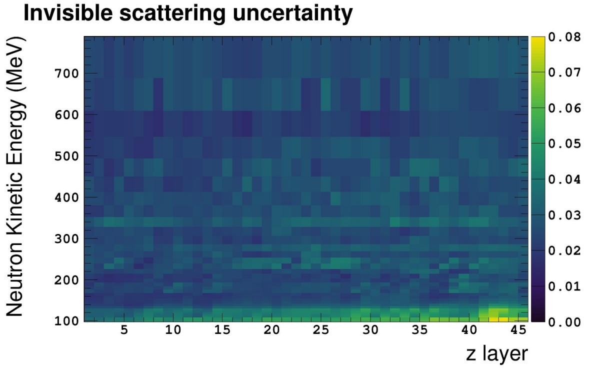

Elastic scattering and inelastic scattering later

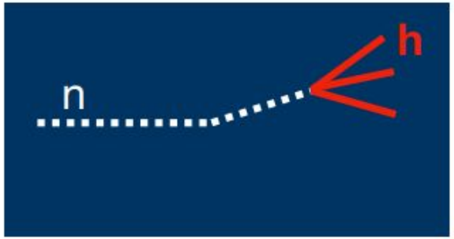

Inelastic scattering with charged particles undetected

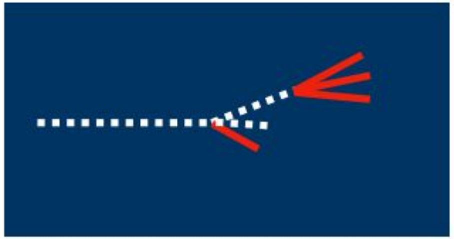

Cross Section Systematics

Detector effects:

- Cube mis-alignment plays a big role: vertical shift of every 5 cube layers by 1 mm causes up 10% difference in event rate between Z layers
- Relatively small contribution from MPPC type differences
- Difference between single-track selection and “no-cut” case propagated as the uncertainty to the event rate in each energy bin and layer

Example of misalignment

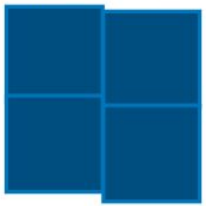

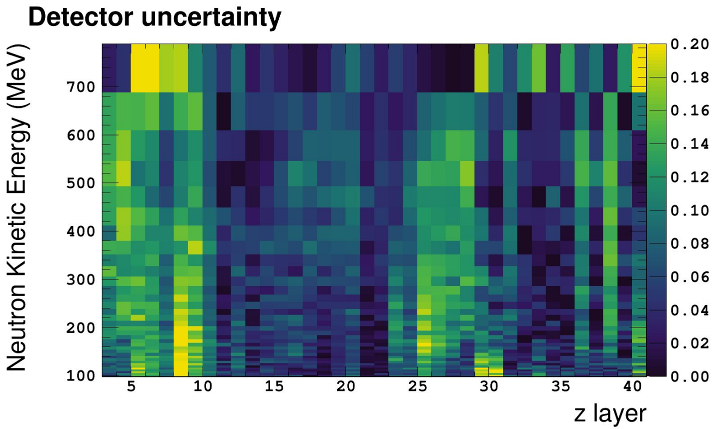

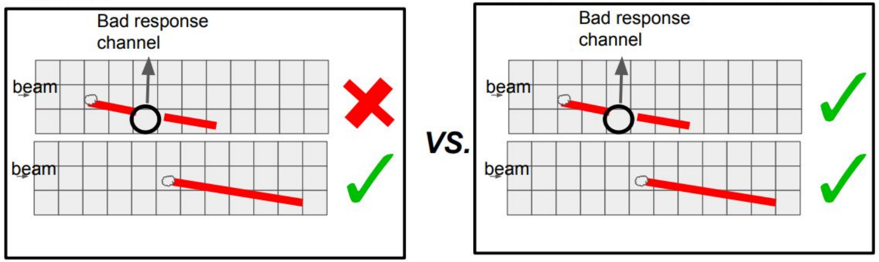

Cross Section Systematics

Light yield:

- Light yield obtained using cosmic data taken at LANL
- Random fluctuation of light yield from nominal propagated as the uncertainty of the event rate in each energy bin and layer

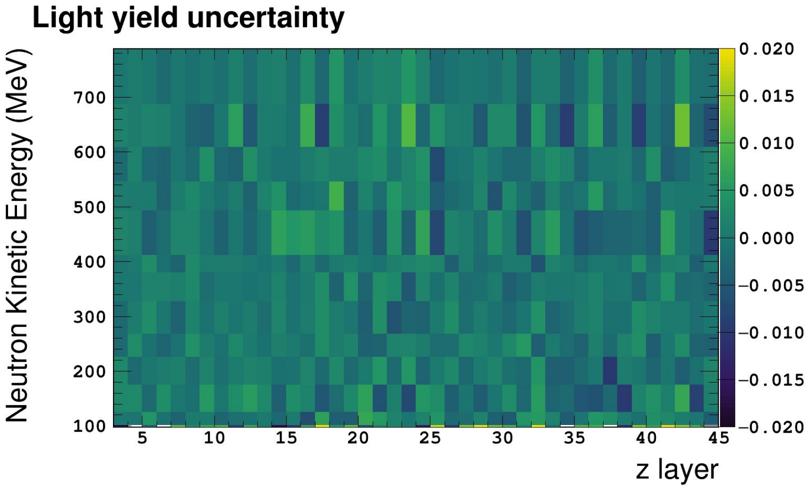

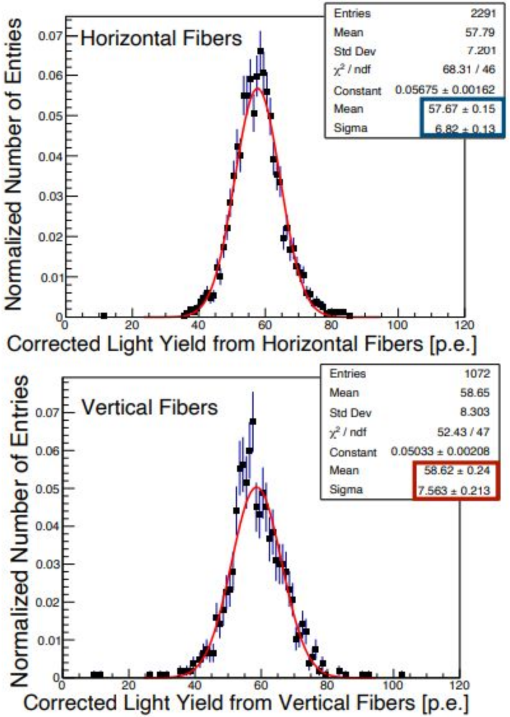

Cross Section Systematics

Geometric acceptance:

- Limited size of our detector can introduce a bias in the single track selection:
  - A multiple-track event can be selected as single track
  - Cut on number of voxels and upper limit on the fitting range (layer 40) used to mitigate this effect
- Data driven method used to estimate such uncertainty:
  - Expand or reduce the detector size by shifting hits boundary
  - Ratio between event rate (energy vs z-layer) with and without boundary is taken as systematic error

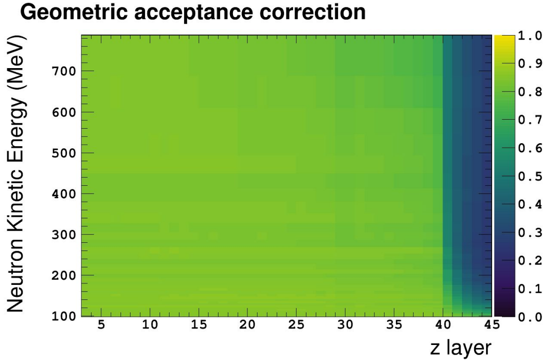

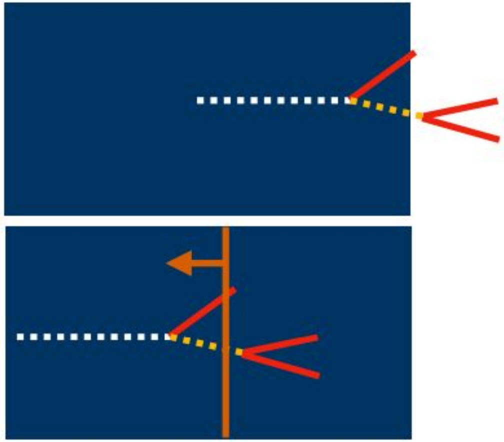

Cross Section Systematics

Collimator interaction:

- Multiple interactions inside the collimators
- None of which interacts in first collimator arrive to the detector while the second can contribute to energy smearing (feed-down bias)
- Smearing the neutron energy using MC estimations of the energy lost by neutrons showed minimal impact

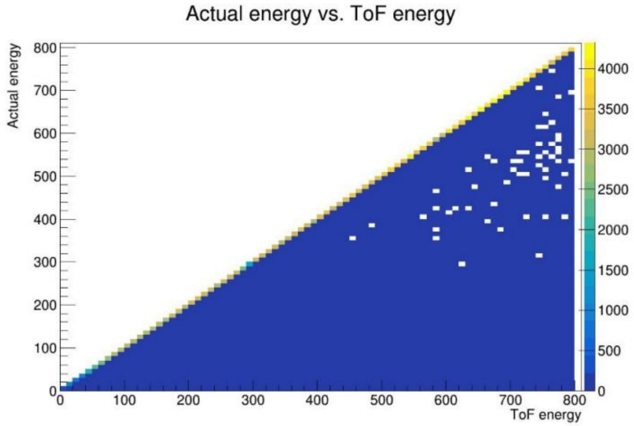

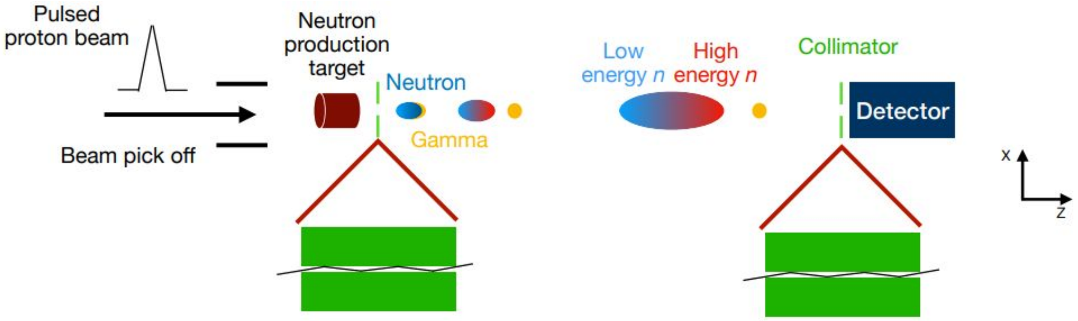

Cross Section Error Propagation

- The systematics that change the number of events in each z-layer are propagated in the following way:
  - Fit with the exponential $N_0 e^{-T\sigma z}$ the distribution obtained after every gaussian variation of the number of events in every z-layer and energy bin
  - Fill an histogram with every value of the cross section
  - The systematic uncertainty is the RMS of this distribution
- Time resolution and the uncertainty due to collimator interactions changes the energy distribution (shape-like systematics) all the others change the normalization (number of events in each Z layer)
- The total systematic uncertainty is the sum in quadrature of each systematic error
- Statistical uncertainty given by square root of number of events in every Z layer

Cross Section Result

- Total of 20 hours of data analyzed
- Total rate is about 1e6 events (total interactions are ~1e8 and efficiency is ~1e-2)
- Energy-integrated (98-688 MeV) cross section is 0.36 ± 0.05 barn with a $\chi2$/d.o.f. of 22.03/38

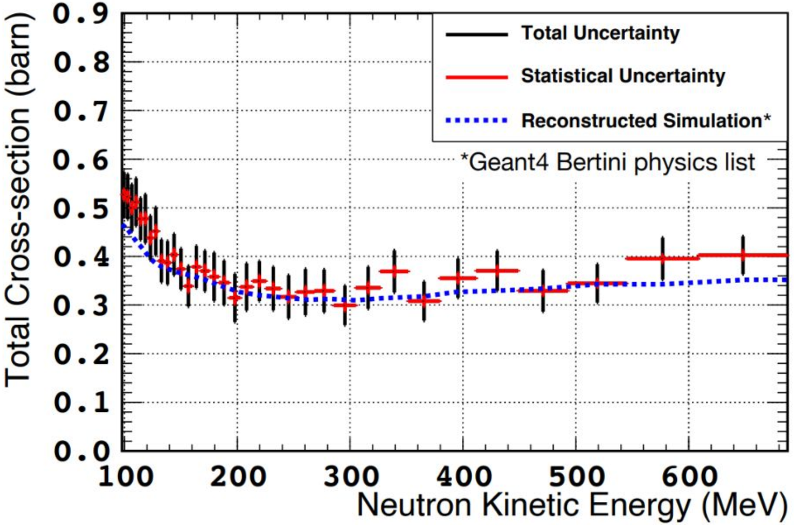

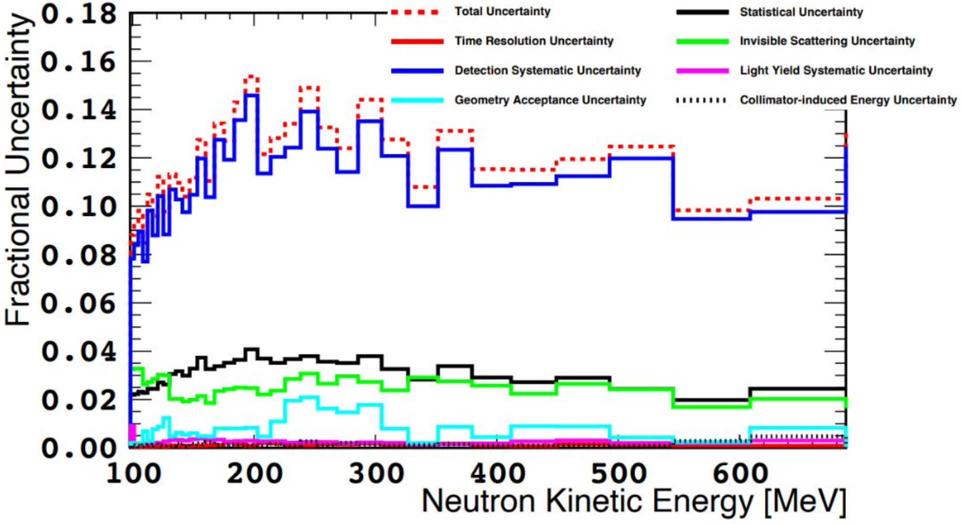

Cross Section Result

- Total of 20 hours of data analyzed
- Total rate is about 1e6 events (total interactions are ~1e8 and efficiency is ~1e-2)
- Energy-integrated (98-688 MeV) cross section is 0.36 ± 0.05 barn with a χ2/d.o.f. of 22.03/38

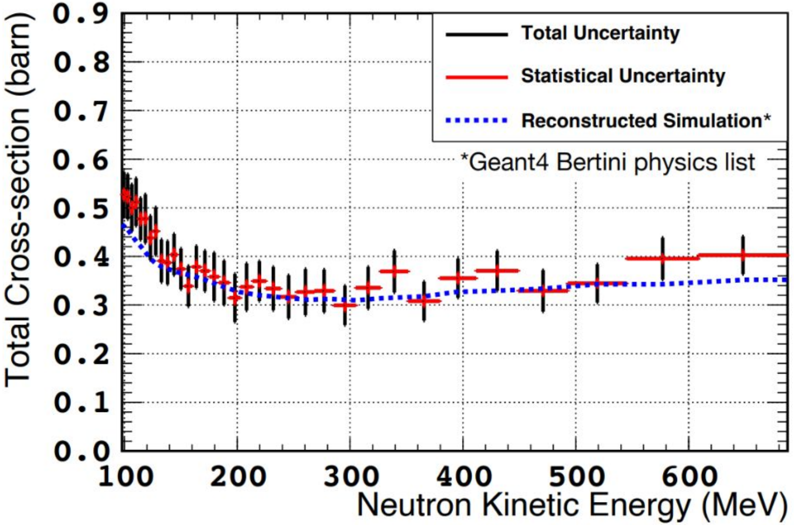

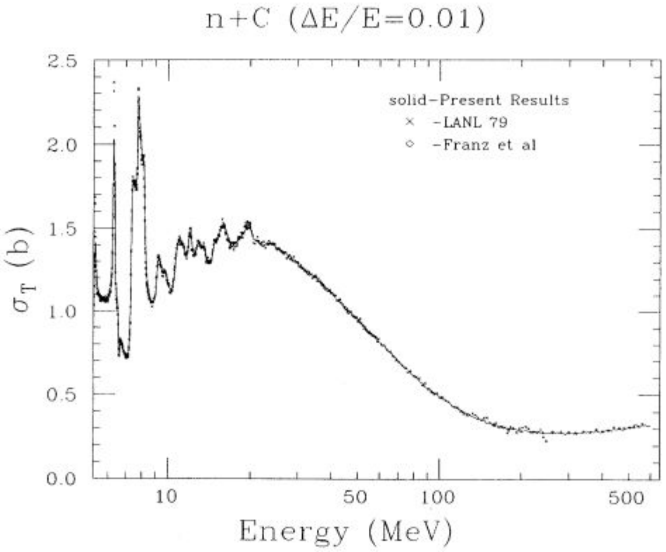

Phys. Rev. C 47, 237 (1993)

On-going Work

- Analysis with neutron beam data taken at LANL in 2020
- Development and testing of electronics system for SuperFGD

LANL 2020

- In 2020, 2 prototype detectors were exposed to the neutron beam at LANL for 2 weeks (same location as 2019)
- 1 was the SuperFGD prototype and another was a smaller prototype (8x8x32 cm3) called the US-Japan prototype which was assembled at SBU
- It uses the final components that will be used in the SuperFGD as well

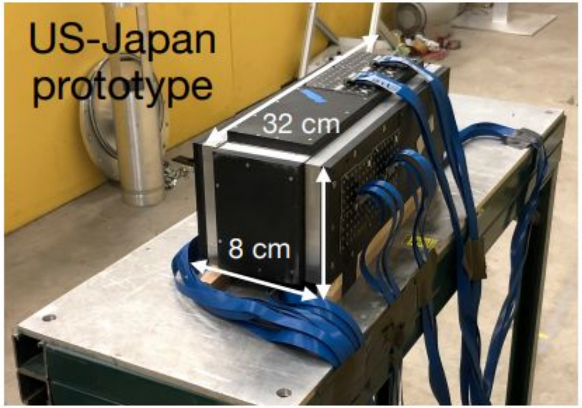

Detector during assembly

LANL 2020

- Different beam configurations: 3.6 μs pulse spacing (1.8 in 2019) to lower the contamination of low energy neutrons in high energy region
- Different detector configurations
- Different collimator size: 1 cm and 1 mm (only 1 cm used in 2019)
- Ongoing studies:
  - Elastic vs inelastic scattering
  - Investigate possibility to constrain invisible scattering
  - Exclusive neutron interaction channel selection
  - Neutron secondary interactions, MC studies and comparison with data

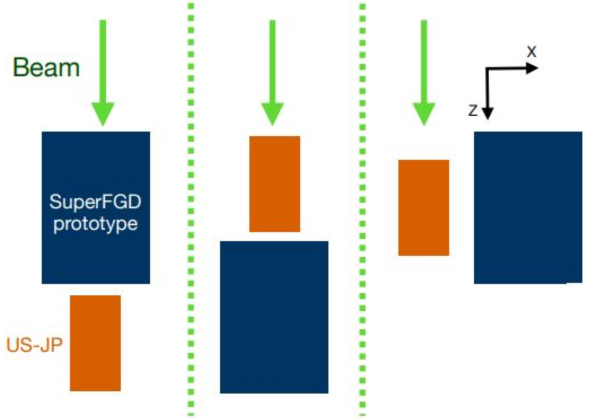

SuperFGD Electronics

- 16 crates to cover around 56000 channels
- 8 crates on each side of the sFGD
- 1 crate has 14 front-end boards (FEB), 1 optical concentrator board (OCB) and 1 backplane

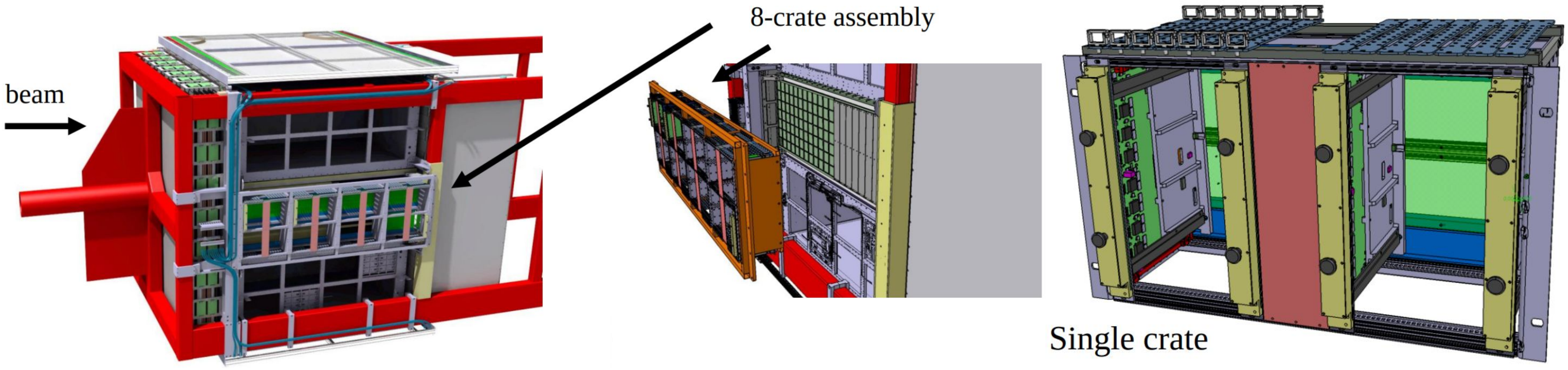

SuperFGD Electronics

sFGD Electronics Architecture

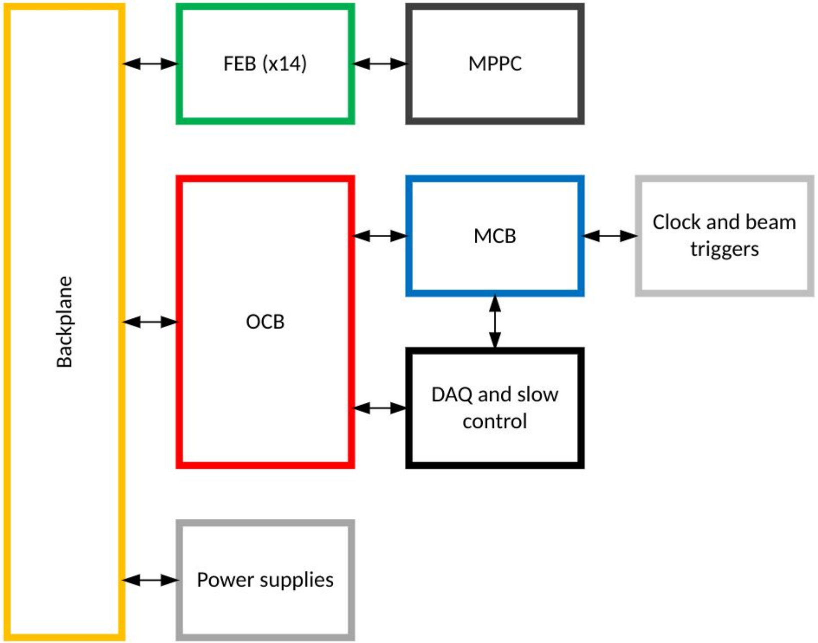

FEB:
Analog processing, ADC, bias voltage to MPPCs (256 channels)

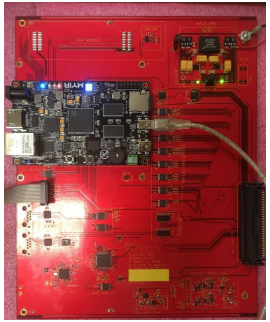

OCB:
Data concatenation, connection to outside world

MCB:
Clock and beam trigger distribution

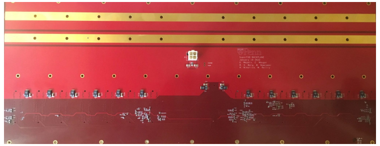

Backplane:
Power and signals distribution

SuperFGD Electronics

- Actively involved in firmware + software development for the OCB
- On-going hardware + firmware tests with key electronic components (crate level)
  - Integration of various SuperFGD electronics components

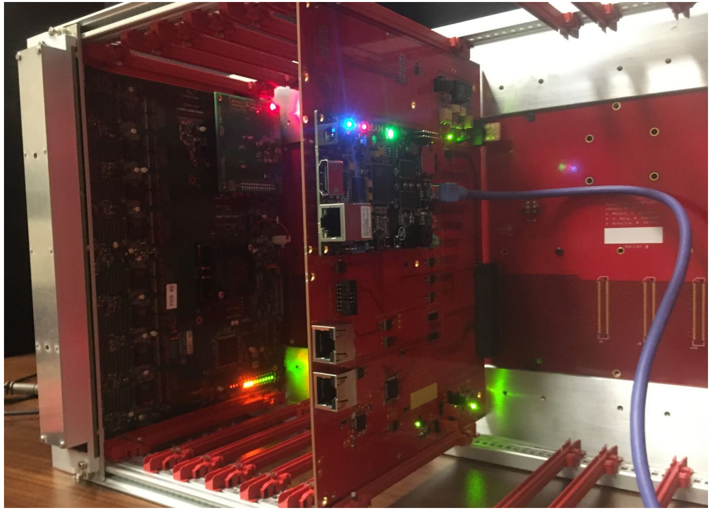

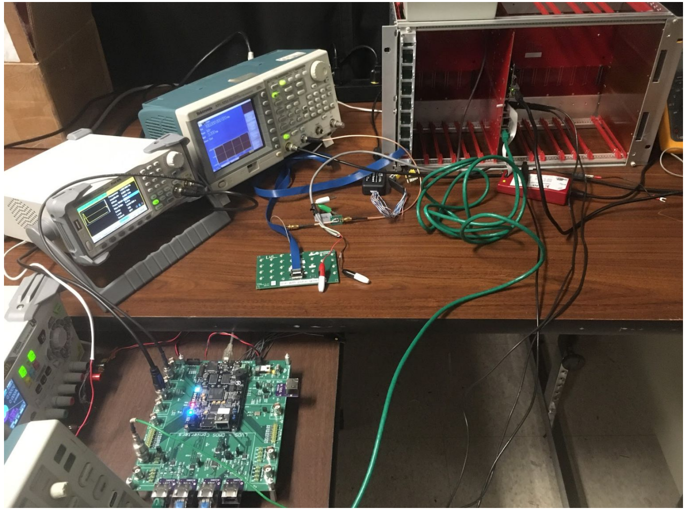

SuperFGD Electronics

- Leading effort in vertical slice test planning of the electronics system for the SuperFGD
    - Effort stated in UPenn and progressing well

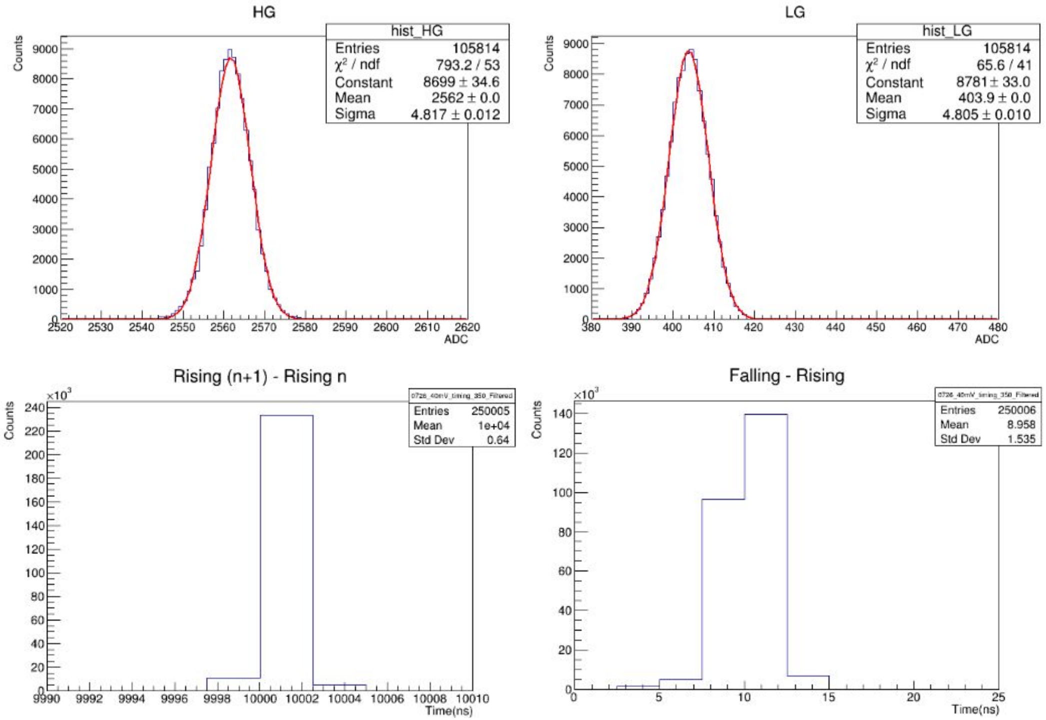

SuperFGD Electronics

- Leading effort in vertical slice test planning of the electronics system for the SuperFGD
  - Effort stated in UPenn and progressing well
  - Full crate test in UniGe in December → Give green light to production of FEBs (x256)
  - Cosmic data taking with SuperFGD electronics + US-Japan prototype

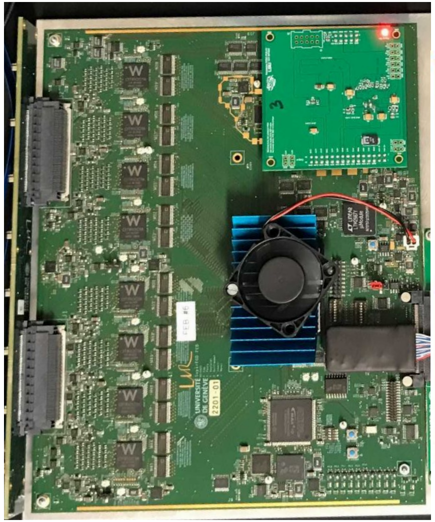

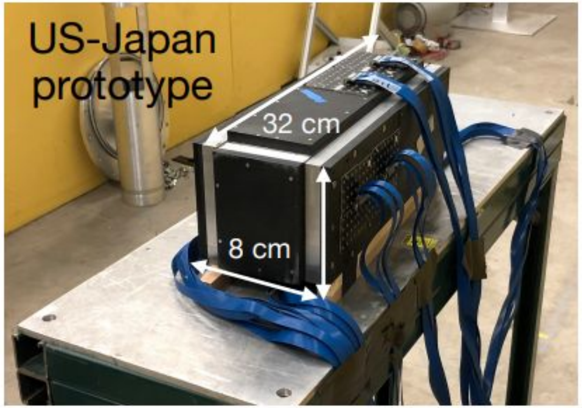

Summary

- Paper on the total n-CH cross section measurement has been submitted on ArXiv and is the first physics results of the technology developed for SuperFGD and 3DST
- It demonstrates the neutron detection capability of the SuperFGD
- Lessons learned from this analysis serve as a lever arm for neutron reconstruction in SuperFGD
    - Detector effects systematic can be more prominent in SuperFGD
    - Needs to be addressed in the analysis of SuperFGD data
- Additional data have been collected with SuperFGD and US-Japan prototypes in 2020 and on-going analysis with the collected data
- Active development and testing with the SuperFGD electronics system
- Lots of interesting physics to be done when the SuperFGD is turned on and collecting neutrino beam data!